

**$J/\psi \rightarrow p\bar{p}\phi$  decay in the isobar resonance model**Jian-Ping Dai,<sup>1,4,\*</sup> Peng-Nian Shen,<sup>6,2,1,5,†</sup> Ju-Jun Xie,<sup>2,3,‡</sup> and Bing-Song Zou<sup>1,2,4,5,§</sup><sup>1</sup>*Institute of High Energy Physics, CAS, Beijing 100049, China*<sup>2</sup>*Theoretical Physics Center for Science Facilities, CAS, Beijing 100049, China*<sup>3</sup>*Department of Physics, Zhengzhou University, Zhengzhou, Henan 450001, China*<sup>4</sup>*Graduate University of Chinese Academy of Sciences, Beijing 100049, China*<sup>5</sup>*Center of Theoretical Nuclear Physics, National Laboratory of Heavy Ion Accelerator, Lanzhou 730000, China*<sup>6</sup>*College of Physics and Technology, Guangxi Normal University, Guilin 541004, China*

(Received 10 October 2011; published 11 January 2012)

Based on the effective Lagrangian approach, the  $J/\psi \rightarrow p\bar{p}\phi$  decay is studied in an isobar resonance model with the assumption that the  $\phi$ -meson is produced from intermediate nucleon resonances. The contributions from the  $N_{1/2}^*(1535)$ ,  $N_{3/2}^*(1900)$ ,  $N_{1/2}^*(2090)$  and  $N_{1/2}^*(2100)$  states are considered. In terms of the coupling constants  $g_{\phi NN^*}^2$  and  $g_{\psi NN^*}^2$  extracted from the reaction cross section of the  $\pi^- p \rightarrow n\phi$  process, and the partial decay widths of the  $J/\psi \rightarrow p\bar{p}\eta$  and  $J/\psi \rightarrow p\bar{n}\pi^-$  processes, respectively, the invariant mass spectrum and the Dalitz plot for  $J/\psi \rightarrow p\bar{p}\phi$  decay are predicted. It is shown that there are two types of results. In the type I case, a large peak structure around 2.09 GeV implies that a considerable amount of  $N\phi$  or  $qqqs\bar{s}$  component may exist in the narrow-width  $N_{1/2}^*(2090)$  state, but a tiny  $qqqs\bar{s}$  component in the broad-width  $N_{1/2}^*(2100)$  state. In the type II case, a small peak around 2.11 GeV may only indicate the existence of a certain amount of  $p\phi$  or  $qqqs\bar{s}$  component in the narrow-width  $N_{1/2}^*(2100)$  state, but no information for the broad-width  $N_{1/2}^*(2090)$  state. Further BESIII data with high statistics would help us to distinguish the strange structures of these  $N^*$ s.

DOI: 10.1103/PhysRevD.85.014011

PACS numbers: 13.75.-n, 13.75.Cs, 14.20.Gk

**I. INTRODUCTION**

In past decades, many excited states of nucleon were observed and their properties, such as the mass, width, decay modes, etc., have more or less accurately been measured. Most of them can be well explained by quark models, but some of them are very difficult to be fitted into the nucleon spectrum predicted by the three-valence-quark models. To explain the discrepancy, aside from the inaccurate and insufficient-statistics data due to the limited experimental techniques and methods, one could speculate that these states may contain some constituents other than three  $u$  ( $d$ ) valence quarks, especially the  $s$  and  $\bar{s}$  quarks. This conjecture can be checked through experiments. In the later experiments, through data analysis, some excited states of nucleon ( $N^*$ ) were indeed found to couple strongly with strange particles. For instance, in the  $J/\psi \rightarrow \bar{p}K^+\Lambda$  decay and  $pp \rightarrow p\Lambda K^+$  reaction [1,2], in the  $\gamma p \rightarrow K^+\Lambda$  process [3–6],  $N^*(1535)$  was found to have a significant strength of coupling to the  $K\Lambda$  channel. This indicates that the  $N^*(1535)$  state may contain a considerable amount of the  $s\bar{s}$  component, which is consistent with a very large branching fraction of 45 ~ 60% for the  $N^*(1535) \rightarrow N\eta$  decay.

On the other hand, the  $\phi$ -meson is mainly composed of  $s\bar{s}$ . According to the Okubo-Zweig-Iizuka rule [7], the production rate of  $\phi$ -meson in the nuclear process would

be suppressed if the initial interacting particles do not contain strange ( $s$ ,  $\bar{s}$ ) constituents. On the contrary, if a  $N^*$  contains strange constituents, its coupling to a channel involving a  $\phi$ -meson might be relatively strong. In fact, it is found that the data on  $pp \rightarrow p\bar{p}\phi$  and  $\pi^- p \rightarrow n\phi$  reaction near  $\phi$ -production threshold can be well explained as long as the coupling constant of  $\phi NN^*(1535)$  is sufficiently large, which implies a considerable amount of  $s\bar{s}$  component in the  $N^*(1535)$  [8]. Therefore, with the accumulation of high statistics data on charmonium decays at BESIII, the  $J/\psi \rightarrow p\bar{p}\phi$  decay would also be a good place to check whether some  $N^*$ s, as the intermediate states in the decay process, have large coupling to  $N\phi$  and hence large strange components.

Similar to  $N^*(1535)$ , some nucleon resonances, which have not yet been well established and cannot be well fitted into the nucleon spectrum of quark models, have remarkable branching fractions in some decay channels involving strange particles, such as  $N\eta$ ,  $\Lambda K$ , etc. For example, the  $N\eta$  branching fractions of  $N^*(2090)$ ,  $N^*(2100)$ , and  $N^*(1900)$  are about 41%, 61%, and 14%, respectively [9]. This implies that these states might have sizable strange constituents, and the effect of such ingredients should show up in the  $J/\psi \rightarrow p\bar{p}\phi$  decay.

In fact, the branching fraction of  $J/\psi \rightarrow p\bar{p}\phi$  was measured by the DM2 Collaboration in 1988 [10]. However, due to insufficient statistics, no resonance information was extracted. Recently, the luminosity of BEPCII has reached over  $3 \times 10^{32} \text{ cm}^{-2} \text{ s}^{-1}$  around  $J/\psi$  peak, a huge amount of  $J/\psi$  events, say  $3 \times 10^9$ , will be accumulated at BESIII in one year. The new data set would offer an

\* daijianping@ihep.ac.cn

† shenpn@ihep.ac.cn

‡ xiejun@ihep.ac.cn

§ zous@ihep.ac.cn

opportunity to study the possible strange ingredient in the nucleon resonances.

Here based on the effective Lagrangian approach, the  $J/\psi \rightarrow p\bar{p}\phi$  decay is studied in an isobar resonance model with the assumption that the  $\phi$ -meson is mainly produced from intermediate nucleon resonances. It is our hope that the information of the strange structures in nucleon resonances, especially those not well established, can be deduced from the forthcoming BESIII data, and this paper could provide a useful reference for the BESIII data analysis.

The paper is organized in the following way. In Sec. II, the theoretical model and formalism are briefly introduced. The results are presented and discussed in Sec. III. And in Sec. IV, a concluding remark is given.

## II. MODEL AND FORMALISM

In the resonance model, the  $J/\psi \rightarrow p\bar{p}\phi$  decay undergoes a two-step process, namely  $J/\psi$  first decays into an intermediate  $\bar{p}N^*$  ( $p\bar{N}^*$ ) state, and then  $N^*$  ( $\bar{N}^*$ ) successively decays into  $\phi$  and  $p$  ( $\bar{p}$ ). Corresponding Feynman diagrams are drawn in Fig. 1, where  $k$ ,  $p_1$ ,  $p_2$ ,  $p_3$ , and  $q$  ( $q'$ ) are the four-momenta of  $J/\psi$ ,  $p$ ,  $\bar{p}$ ,  $\phi$ , and  $N^*$  ( $\bar{N}^*$ ), respectively. Although the  $p\phi$  invariant mass is limited to be from  $m_p + m_\phi$  to  $m_{J/\psi} - m_{\bar{p}}$ , i.e.,  $1.96 \sim 2.15$  GeV, due to the phase space restriction, the embedded intermediate  $N^*$  states may have masses within or outside this range. Some  $N^*$  states with masses slightly outside this mass range may also contribute significantly through their off-shell propagation if they have large coupling to  $p\phi$ . For minimizing our calculation without affecting qualitative conclusions, in the present approach, we only consider those intermediate  $N^*$  states which may give large contribution according to available information. Thus, the adopted  $N^*$  state should have the following features: It should have a relatively large branching fraction for a decay in which strange particles are involved. Thus, it might have a configuration with strangeness, so that it would be easier decaying into  $N\phi$  and relatively important in the  $J/\psi \rightarrow p\bar{p}\phi$  decay. It would also be reasonable that the spin of the  $N^*$  state is  $\leq 5/2$  only due to the limited phase space from  $J/\psi$  decays. In the practical calculation, in the mass region above the  $p\phi$  threshold, we only consider the  $N_{1/2}^*(2090)S_{11}$  and  $N_{1/2}^*(2100)P_{11}$  states whose

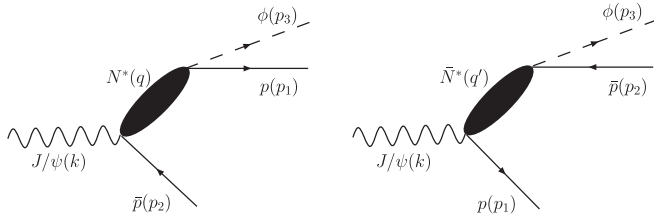


FIG. 1. Feynman diagrams for the  $J/\psi \rightarrow p\bar{p}\phi$  decay in the resonance model.

branching fractions for the  $N\eta$  channel are about 0.41 and 0.61, respectively, although the contribution from the later one would subject to a  $p$ -wave suppression, and ignore  $N_{3/2}^*(2080)D_{13}$  and  $N_{5/2}^*(2000)F_{15}$  because of their tiny branching fractions for  $N\eta$  (about 0.03). For the subthreshold  $N^*$  resonances, we only take  $N_{1/2}^*(1535)S_{11}$  and  $N_{3/2}^*(1900)P_{13}$  into account due to their large  $N\eta$  branching fractions of about 0.45–0.60 and 0.14, respectively. The reason for disregarding other subthreshold  $N^*$  resonances is because of their much smaller branching fractions to the channels involving strangeness, such as  $N\eta$  and  $\Lambda K$ . Based on such consideration and the results given by the partial wave analysis for the  $N^*$  production from  $J/\psi$  decays in Refs. [11,12], we can safely assume that among known resonances only  $N_{1/2}^*(1535)S_{11}$ ,  $N_{3/2}^*(1900)P_{13}$ ,  $N_{1/2}^*(2090)S_{11}$  and  $N_{1/2}^*(2100)P_{11}$  may give significant contribution to the  $J/\psi \rightarrow p\bar{p}\phi$  process. For simplicity, we omit the spectroscopic symbol in the notation of the  $N^*$  state hereafter.

To reveal the decay property of the  $J/\psi \rightarrow p\bar{p}\phi$  process, the coupling constants  $g_{\phi NN^*}$  and  $g_{\psi NN^*}$  should be fixed at the beginning.

### A. Determination of $g_{\phi NN^*}^2$

As mentioned in Ref. [8], the  $\phi$ -meson production near the  $n\phi$  threshold in the  $\pi^- p \rightarrow n\phi$  reaction is dominated by the intermediate nucleon resonances in the  $s$  channel, and the effects from the  $u$ -channel  $N^*$  exchange and the  $t$ -channel  $\rho$ -meson exchange between pion and proton are found to be negligible, although in some references the  $t$ -channel  $\rho$ -meson exchange and/or nucleon pole contributions were assumed to be important [8,13]. Based on this argument, the coupling constant  $g_{\phi NN^*}^2$  can be extracted by fitting the cross section data of the  $\pi^- p \rightarrow n\phi$  reaction in the resonance model [8,14]. The  $s$ -channel Feynman diagram for such a process is shown in Fig. 2, where  $p_1$ ,  $p_2$ ,  $p_3$ ,  $p_4$ , and  $q$  denote the four-momenta of the incoming  $\pi^-$  and proton, outgoing  $\phi$  and neutron, and intermediate  $N^*$ , respectively. In this diagram, the coupling constant  $g_{\pi NN^*}^2$  ( $g_{\eta NN^*}^2$ ) can be determined in terms of a commonly used effective Lagrangian [8,15,16]. The effective Lagrangian of the  $\pi NN^*$  coupling for a nucleon resonance with spin-parity  $J_{N^*}^P = \frac{1}{2}^-$  can be written as [8,15,16]

$$\mathcal{L}_{\pi NN^*} = g_{\pi NN^*} \bar{N}^* \vec{\tau} \cdot \vec{\pi} N + \text{H.c.}, \quad (1)$$

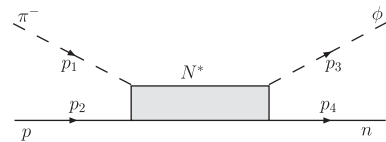


FIG. 2.  $s$ -channel Feynman diagram for the  $\pi^- p \rightarrow n\phi$  reaction in the resonance model.

with  $J_{N^*}^P = \frac{1}{2}^+$

$$\mathcal{L}_{\pi NN^*} = ig_{\pi NN^*} \bar{N}^* \gamma_5 \vec{\tau} \cdot \vec{\pi} N + \text{H.c.}, \quad (2)$$

and with  $J_{N^*}^P = \frac{3}{2}^+$ , say  $N^*(1900)$ , [15]

$$\mathcal{L}_{\pi NN^*} = i \frac{g_{\pi NN^*}}{M_{N^*}} \bar{N}^* \mu \vec{\tau} \cdot \partial_\mu \vec{\pi} N + \text{H.c.}, \quad (3)$$

where  $g_{\pi NN^*}$ ,  $N^{*\mu}$ ,  $N$ ,  $\vec{\pi}$  and  $\vec{\tau}$  denote the coupling constant of a pion to a nucleon and a  $N^*$ , the Rarita-Schwinger field of  $N^*$  with its spin of 3/2 and mass of  $M_{N^*}$ , the field of nucleon, the field of  $\vec{\pi}$  and the isospin matrices, respectively. And the effective Lagrangian for the  $\eta NN^*(1535)$  coupling can be expressed as

$$\mathcal{L}_{\eta NN^*} = g_{\eta NN^*} \bar{N}^* \eta N + \text{H.c.} \quad (4)$$

With these Lagrangians, the partial decay widths of the  $N^*$  states can easily be derived by evaluating the transition rate from the initial  $N^*$  state to the final  $N\pi(N\eta)$  state

$$\Gamma_{N^*(1535) \rightarrow N\pi(\eta)} = \frac{3g_{\pi(\eta)NN^*}^2 (m_N + E_N^{\text{cm}}) p_N^{\text{cm}}}{4\pi M_{N^*}}, \quad (5)$$

$$\Gamma_{N^*(1900) \rightarrow N\pi} = \frac{g_{\pi NN^*}^2 (m_N + E_N^{\text{cm}}) (p_N^{\text{cm}})^3}{4\pi M_{N^*}^3}, \quad (6)$$

$$\Gamma_{N^*(2090) \rightarrow N\pi} = \frac{3g_{\pi NN^*}^2 (m_N + E_N^{\text{cm}}) p_N^{\text{cm}}}{4\pi M_{N^*}}, \quad (7)$$

$$\Gamma_{N^*(2100) \rightarrow N\pi} = \frac{3g_{\pi NN^*}^2 (E_N^{\text{cm}} - m_N) p_N^{\text{cm}}}{4\pi M_{N^*}}, \quad (8)$$

with  $E_N^{\text{cm}}$  and  $p_N^{\text{cm}}$  as the energy and momentum of the nucleon in the  $N^*$  at-rest frame.

From the measured  $\pi N$  ( $\eta N$ ) branching fractions of the  $N^*$  state [9], the effective coupling constants  $g_{\pi NN^*}^2$  ( $g_{\eta NN^*}^2$ ) can be extracted.

The effective Lagrangians of the  $\phi NN^*$  interaction for various  $N^*$  states are as follows [8].

For a  $N^*$  with  $J_{N^*}^P = \frac{1}{2}^-$ , say  $N^*(1535)$  or  $N^*(2090)$ ,

$$\mathcal{L}_{\phi NN^*} = g_{\phi NN^*} \bar{N}^* \gamma_5 \left( \gamma_\mu - \frac{q_\mu \not{q}}{q^2} \right) \Phi^\mu N + \text{H.c.} \quad (9)$$

with  $q$  being the four-momentum of  $N^*$  and  $\Phi^\mu$  being the field of the  $\phi$  meson.

For a  $N^*$  with  $J_{N^*}^P = \frac{1}{2}^+$ , say  $N^*(2100)$ ,

$$\mathcal{L}_{\phi NN^*} = g_{\phi NN^*} \bar{N}^* \gamma_\mu \Phi_\phi^\mu N + \text{H.c.}, \quad (10)$$

and for a  $N^*$  with  $J_{N^*}^P = \frac{3}{2}^+$ , say  $N^*(1900)$ , [15]

$$\mathcal{L}_{\phi NN^*} = ig_{\phi NN^*} \bar{N}^* \gamma_5 \Phi_\phi^\mu N + \text{H.c.} \quad (11)$$

For the off-shell effect of  $N^*$ , a form factor

$$F_{N^*}(q^2) = \frac{\Lambda^4}{\Lambda^4 + (q^2 - M_{N^*}^2)^2} \quad (12)$$

with  $\Lambda$  being the cutoff parameter is introduced for the  $MNN^*$  vertex [17,18].

The propagator  $G_J(q)$  of a  $N_J^*$  with momentum  $q$  can be written in a Breit-Wigner form [19]. For a  $J_{N^*} = 1/2$  state,

$$G_{(1/2)}(q) = \frac{i(\pm \not{q} + M_{N^*})}{q^2 - M_{N^*}^2 + iM_{N^*}\Gamma_{N^*}}. \quad (13)$$

For a  $J_{N^*} = 3/2$  state,

$$G_{(3/2)}^{\mu\nu}(q) = \frac{i(\pm \not{q} + M_{N^*})}{q^2 - M_{N^*}^2 + iM_{N^*}\Gamma_{N^*}} \left( -g^{\mu\nu} + \frac{1}{3}\gamma_\mu \gamma_\nu \right. \\ \left. + \frac{1}{3M_{N^*}}(\gamma^\mu q^\nu - \gamma^\nu q^\mu) + \frac{2}{3M_{N^*}}q^\mu q^\nu \right). \quad (14)$$

In above two equations, the upper and lower signs in  $\pm$  and  $\mp$  are for particle and antiparticle, respectively.

Based on these effective Lagrangians, form factors and propagators, we can write the  $s$ -channel invariant amplitude due to an intermediate  $N^*$  state in the  $\pi^- p \rightarrow n\phi$  reaction as

$$\mathcal{M}_{N^*} \propto \sqrt{2} g_{\pi NN^*} g_{\phi NN^*} F_{N^*}(q^2) \bar{u}(p_n, s_n) \Gamma_{\phi NN^*} \varphi_\phi(p_\phi, s_\phi) \\ \times G_{N^*}(q) \varphi_\pi(p_\pi) \Gamma_{\pi NN^*} u(p_p, s_p), \quad (15)$$

where  $u$ ,  $\varphi_\phi$  and  $\varphi_\pi$  denote the fields of the nucleon,  $\phi$ -meson and  $\pi$ -meson, respectively,  $p_n$ ,  $p_p$ ,  $p_\phi$ , and  $p_\pi$  represent the momenta of the proton, neutron,  $\phi$ -meson, and  $\pi$ -meson, respectively,  $s_n$ ,  $s_p$  and  $s_\phi$  describe the spins of the proton, neutron and  $\phi$ -meson, respectively, and  $\Gamma_{\phi NN^*}$  and  $\Gamma_{\pi NN^*}$  stand for the vertex functions of  $\phi NN^*$  and  $\pi NN^*$ , respectively. Adding up the amplitudes for all the  $N^*$ 's considered, we obtain the total invariant amplitude

$$\mathcal{M}_{\pi^- p \rightarrow n\phi} = \sum_{N^*} \mathcal{M}_{N^*}, \quad (16)$$

where  $N^*$  runs over all the considered states. Consequently, we can calculate the total cross section of the  $\pi^- p \rightarrow n\phi$  reaction by using the following equation:

$$\sigma = \int d\Phi_2(\mathbb{P}, p_p, p_\pi, p_n, p_\phi) \frac{(2\pi)^4}{F} |\mathcal{M}_{\pi^- p \rightarrow n\phi}|^2, \quad (17)$$

with the flux factor

$$F = 4\sqrt{(p_p \cdot p_\pi)^2 - m_p^2 m_\pi^2}, \quad (18)$$

$d\Phi_2$  being an element of the two-body phase space, and  $\mathbb{P}$  being the total momentum of the system. By using extracted  $g_{\pi NN^*}^2$  values and adjusting  $g_{\phi NN^*}^2$ 's to fit the total cross section of the  $\pi^- p \rightarrow n\phi$  reaction, we can obtain phenomenological magnitudes for  $g_{\phi NN^*}^2$ 's.

### B. Determination of $g_{\psi NN^*}^2$

The coupling constants  $g_{\psi NN^*}^2$  can be extracted from the BESII data for the  $J/\psi \rightarrow p\bar{n}\pi^-$  and  $J/\psi \rightarrow p\bar{p}\eta$  decays [11,12]. The Feynman diagrams for these decays are the same as those in Fig. 1 except that the  $\phi$ -meson is replaced with the  $\pi$ - and  $\eta$ -mesons, respectively.

The effective Lagrangian for the  $J/\psi NN^*$  interaction can be chosen in the following form. For a  $N^*$  with  $J_{N^*}^P = \frac{1}{2}^-$ , say  $N^*(1535)$  or  $N^*(2090)$ , [1]

$$\mathcal{L}_{\psi NN^*} = ig_{\psi NN^*} \bar{N}^* \gamma_5 \sigma_{\mu\nu} p_\psi^\nu \epsilon^\mu(\vec{p}_\psi, s_\psi) N + \text{H.c.} \quad (19)$$

with  $p_\psi$  and  $\epsilon(p_\psi)$  being the four-momentum and the polarization vector of  $J/\psi$ , respectively, for a  $N^*$  with  $J_{N^*}^P = \frac{1}{2}^+$ , say  $N^*(2100)$ ,

$$\mathcal{L}_{\psi NN^*} = g_{\psi NN^*} \bar{N}^* \gamma_\mu \epsilon^\mu(\vec{p}_\psi, s_\psi) N + \text{H.c.}, \quad (20)$$

and for a  $N^*$  with  $J_{N^*}^P = \frac{3}{2}^+$ , say  $N^*(1900)$ , [15]

$$\mathcal{L}_{\psi NN^*} = ig_{\psi NN^*} \bar{N}^* \gamma_5 \epsilon^\mu(\vec{p}_\psi, s_\psi) N + \text{H.c.} \quad (21)$$

It should be mentioned that  $J/\psi$  meson produced in BEPCII is transversely polarized, namely  $s_\psi = \pm 1$ . The completeness condition of polarization vector obeys

$$\sum_{s=\pm 1} \epsilon_\mu(\vec{p}, s) \epsilon_\nu^*(\vec{p}, s) = \delta_{\mu\nu} (\delta_{\mu 1} + \delta_{\mu 2}). \quad (22)$$

Then, the invariant decay amplitude due to a specific  $N^*$  in the  $J/\psi \rightarrow p\bar{n}\pi^-$  ( $J/\psi \rightarrow p\bar{p}\eta$ ) decay can easily be written as

$$\begin{aligned} \mathcal{M}_{N^*} &\propto \xi g_{\pi(\eta) NN^*} g_{\psi NN^*} F_{N^*}(q^2) \bar{u}(p_p, s_p) \\ &\quad \times \Gamma_{\pi(\eta) NN^*} \varphi_{\pi(\eta)}(p_{\pi(\eta)}) G_{N^*}(q) \varphi_\psi(p_\psi, s_\psi) \\ &\quad \times \Gamma_{\psi NN^*} v(p_{\bar{p}}, s_{\bar{p}}), \end{aligned} \quad (23)$$

with  $u$  ( $v$ ) being the field of proton (antiproton),  $\varphi_\psi$  and  $\varphi_{\pi(\eta)}$  being the fields of  $\psi$  and  $\pi(\eta)$ , respectively,  $p_p, p_{\bar{p}}$  and  $p_\psi$  being the momenta of the particles labeled in the corresponding subscript, respectively,  $s_p, s_{\bar{p}}$  and  $s_\psi$  being the spins of the corresponding particles, respectively, and  $\Gamma_{\pi(\eta) NN^*}$  and  $\Gamma_{\psi NN^*}$  being the vertex functions of  $\pi(\eta) NN^*$  and  $\psi NN^*$ , respectively. The coefficient  $\xi$  is taken to be  $\sqrt{2}$  for the  $p\bar{n}\pi^-$  reaction, but 1 for the  $p\bar{p}\eta$  reaction. Then, the total invariant amplitude can be obtained by summing over all possible  $N^*$  states

$$\mathcal{M}_{J/\psi \text{ decay}} = \sum_{N^*} \mathcal{M}_{N^*}. \quad (24)$$

And the partial decay width of  $J/\psi \rightarrow p\bar{n}\pi^-$  ( $J/\psi \rightarrow p\bar{p}\eta$ ) can be calculated by

$$\begin{aligned} d\Gamma &= \frac{1}{2} \frac{(2\pi)^{-5} p_p^0 d^3 p_p p_{\bar{p}}^0 d^3 p_{\bar{p}} d^3 p_{\pi(\eta)}}{2 M_\psi p_{\pi(\eta)}^0} \sum_{s_\psi} \sum_{s_p, s_{\bar{p}}} |\mathcal{M}_{J/\psi \text{ decay}}|^2 \\ &\quad \times \delta^4(p_\psi - p_p - p_{\bar{p}} - p_{\pi(\eta)}). \end{aligned} \quad (25)$$

By fitting the branching fractions of  $(2.09 \pm 0.18) \times 10^{-3}$  for  $J/\psi \rightarrow p\bar{n}\pi^-$  and  $(2.12 \pm 0.09) \times 10^{-3}$  for  $J/\psi \rightarrow p\bar{p}\eta$  [9], respectively, the magnitude of  $g_{\psi NN^*}^2$  can be extracted.

### C. $J/\psi \rightarrow p\bar{p}\phi$ decay

Using the effective Lagrangians mentioned above, the invariant amplitude of the  $J/\psi \rightarrow p\bar{p}\phi$  decay can easily be derived. Its form is the same as that in Eq. (23) except that  $\pi$  is substituted with  $\phi$

$$\begin{aligned} \mathcal{M}_{N^*} &\propto g_{\phi NN^*} g_{\psi NN^*} F_{N^*}(q^2) \bar{u}(p_p, s_p) \Gamma_{\phi NN^*} \varphi_\phi(p_\phi, s_\phi) \\ &\quad \times G_{N^*}(q) \varphi_\psi(p_\psi, s_\psi) \Gamma_{\psi NN^*} v(p_{\bar{p}}, s_{\bar{p}}). \end{aligned} \quad (26)$$

Then, the total invariant amplitude can be obtained by summing over the contributions from all possible  $N^*$  states

$$\mathcal{M}_{J/\psi \rightarrow p\bar{p}\phi} = \sum_{N^*} \mathcal{M}_{N^*}, \quad (27)$$

The invariant mass spectrum of  $p\phi$  in the  $J/\psi \rightarrow p\bar{p}\phi$  decay can be expressed as [9]

$$\frac{d\Gamma}{d\Omega_p^* d\Omega_{\bar{p}}} = \frac{1}{2} \frac{1}{(2\pi)^5} \frac{(2m_p)^2}{16M_\psi^2} |\mathcal{M}|^2 |p_p^*| |\bar{p}| dm_{p\phi}, \quad (28)$$

where ( $|p_p^*|, \Omega_p^*$ ) are the momentum of proton in the rest frame of  $p$  and  $\phi$ , respectively, and  $\Omega_{\bar{p}}$  is the angle of antiproton in the rest frame of the decaying  $J/\psi$ . Integrating over all the angles in the rest frame of  $J/\psi$ , the Dalitz plot can be derived in the following form [9]:

$$d\Gamma = \frac{1}{2} \frac{1}{(2\pi)^3} \frac{(2m_p)^2}{32M_\psi^3} |\mathcal{M}|^2 dm_{p\phi}^2 dm_{\bar{p}\phi}^2, \quad (29)$$

with  $m_{p(\bar{p})\phi}$  the invariant mass of  $p(\bar{p})$  and  $\phi$ .

## III. RESULTS AND DISCUSSION

Based on previous discussions, only  $N_{1/2}^*(1535)$ ,  $N_{3/2}^*(1900)$ ,  $N_{1/2}^*(2090)$  and  $N_{1/2}^*(2100)$  are included in our concrete calculation. The extracted  $g_{\pi NN^*}^2$  and  $g_{\eta NN^*}^2$  for each  $N^*$  are tabulated in Table I. It should be noted that the total width and the branching fractions of  $N_{S_{11}}^*(1535)$  (or the partial decay widths) for the  $N\pi$  and  $N\eta$  channels have more or less accurately been measured, thus  $g_{\pi NN^*(1535)}^2$  and  $g_{\eta NN^*(1535)}^2$  can be estimated by using the averaged values of branching fractions given in PDG [9]. However, for the two-star state  $N_{3/2}^*(1900)$  and one-star states  $N_{1/2}^*(2090)$  and  $N_{1/2}^*(2100)$ , their partial decay widths for the  $N\pi$  channel have not precisely been confirmed yet. The extracted  $g_{\pi NN^*}^2$  would be allowed to change in a range due to the mentioned large uncertainty. The range can roughly be estimated by using the maximal and minimal values [9] of the total width and the  $N\pi$  branching fraction for the corresponding  $N^*$ .



TABLE I. Coupling constants  $g_{\pi NN^*}^2$  and  $g_{\eta NN^*}^2$  for various  $N^*$  states. Experimental data are adopted from [9].

$N^*$	$\Gamma_{\text{tot}}$ (GeV)	Decay mode	$\Gamma_{N\pi(\eta)}/\Gamma_{\text{tot}}$	$\Gamma_{N\pi(\eta)}$ (GeV)	$g_{\pi(\eta)NN^*}^2$
$N^*(1535)$	0.150	$N\pi$	45%	$0.675 \times 10^{-1}$	0.468
	0.150	$N\eta$	53%	$0.795 \times 10^{-1}$	$0.431 \times 10^1$
$N^*(1900)$	0.180	$N\pi$	5.5%	$0.990 \times 10^{-2}$	$0.113 \times 10^1$
	0.498	$N\pi$	26%	0.129	$0.147 \times 10^2$
$N^*(2090)$	0.095	$N\pi$	9.0%	$0.855 \times 10^{-2}$	$0.410 \times 10^{-1}$
	0.350	$N\pi$	18%	$0.630 \times 10^{-1}$	0.305
	0.414	$N\pi$	10%	$0.414 \times 10^{-1}$	0.200
$N^*(2100)$	0.113	$N\pi$	15%	$0.170 \times 10^{-1}$	0.564
	0.200	$N\pi$	10%	$0.200 \times 10^{-1}$	0.666
	0.260	$N\pi$	12%	$0.312 \times 10^{-1}$	$0.104 \times 10^1$

Then the coupling constants  $g_{\phi NN^*}$  for various  $N^*$ 's can be extracted by fitting the total cross section data for the  $\pi^- p \rightarrow n\phi$  reaction. To consider the off-shell effect of  $N^*$ , form factors as in Eq. (12) with cutoff parameter  $\Lambda$  of 1.8 GeV for  $N_{1/2^-}^*(1535)$  and 2.3 GeV for  $N_{3/2^+}^*(1900)$ ,  $N_{1/2^-}^*(2090)$  and  $N_{1/2^+}^*(2100)$  are employed.

Because of the large uncertainties of  $g_{\pi NN^*}^2$  for the  $N_{3/2^+}^*(1900)$ ,  $N_{1/2^-}^*(2090)$  and  $N_{1/2^+}^*(2100)$  states, we try various possible combinations of  $g_{\pi NN^*}^2$  values for these  $N^*$ 's to fit the reaction data. The results show that two types of combinations give the best fit. The type I demands a smaller total width for  $N_{1/2^-}^*(2090)$  and a larger total width for  $N_{1/2^+}^*(2100)$ , and the type II is the other way round. To be specific, the allowed combinations of total widths for the  $N_{3/2^+}^*(1900)$ ,  $N_{1/2^-}^*(2090)$  and  $N_{1/2^+}^*(2100)$  are as follows:  $\Gamma_{N^*(1900)}/\Gamma_{N^*(2090)}/\Gamma_{N^*(2100)} = 180/95/200$  (MeV), 180/95/260 (MeV), 498/95/200 (MeV), 498/95/260 (MeV) in type I, and 180/350/113 (MeV), 180/414/113 (MeV), 498/350/113 (MeV) and 498/414/113 (MeV) in type II.

The typical fitted curves of these two types are plotted in Figs. 3(a) and 3(b) with  $\chi^2$  being 3.62 and 3.05, respectively. In these figures, the dashed, dotted, dash-dotted, and dash-double-dotted curves denote the contributions from individual  $N_{1/2^-}^*(1535)$ ,  $N_{3/2^+}^*(1900)$ ,  $N_{1/2^-}^*(2090)$  and  $N_{1/2^+}^*(2100)$  states, respectively, the solid curve describes the final fitting result which is obtained by summing over the contributions from all the  $N^*$  states coherently. In order to see the detailed character of the interference contribution with respect to the energy, the contributions from interferences between different  $N^*$ 's to the total cross section in these cases are also plotted in linear plots, Figs. 3(c) and 3(d), respectively. In the figures, only the contributions from the interference term between  $N_{1/2^-}^*(1535)$  and  $N_{1/2^-}^*(2090)$  and the sum of the contributions from the rest of interference terms are given, shown as the solid and dashed curves, respectively, because the former is much larger than the later.

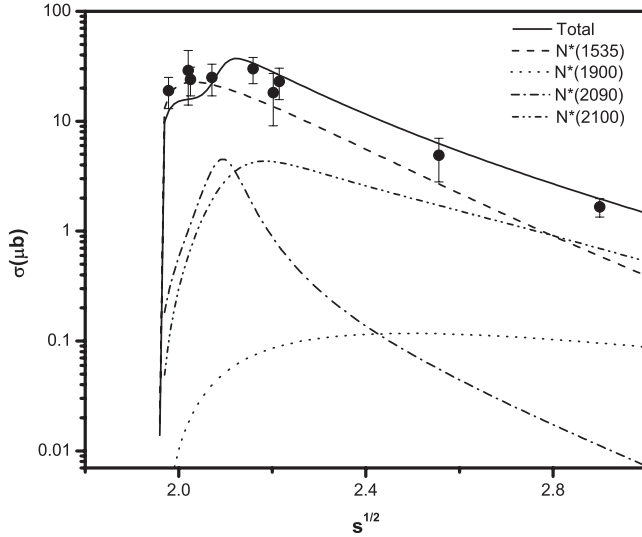
From Fig. 3, we find that  $N_{1/2^-}^*(1535)$  provides a major contribution in the whole energy range considered, especially near the  $N\phi$  threshold. The contribution from  $N_{3/2^+}^*(1900)$  is relatively flat in the high energy region. The cross section from  $N_{1/2^-}^*(2090)$  or  $N_{1/2^+}^*(2100)$  has large uncertainty. Its shape depends on the total width of the state,  $\Gamma_{N^*}$ . If  $\Gamma_{N^*}$  is small, the cross section curve would show a relatively narrow peak around the mass of the  $N^*$ , otherwise it presents a broad structure. This is simply because that a Breit-Wigner form for the  $N^*$  propagator is adopted in the calculation. The  $P$  wave  $N_{1/2^+}^*(2100)$  state can only play a minor role although it has a large branching fraction to  $N\eta$ , since its contribution near the  $N\phi$  threshold is too small. Furthermore, the contribution from  $N^*(2090)$  cannot be large because of a counter contribution from the interference term between  $N^*(2090)$  and  $N^*(1535)$  in the region close to the  $N\phi$  threshold, namely, a larger contribution from  $N^*(2090)$  makes the fit worse. In conclusion, although some higher resonances are introduced, the dominate contribution in the  $\pi^- p \rightarrow n\phi$  cross section still comes from the  $N_{1/2^-}^*(1535)$  state, which is consistent with discussion in Ref. [8]. Thus, the assumption that the contribution from ignored  $N^*$ 's, including their interference terms is about 10 ~ 15% of the total would be reasonable, and arranging the contributions from mentioned four  $N^*$ 's in a range of 85 ~ 90% of the total will not affect our qualitative conclusion.

Based on the best fit, namely, a small enough  $\chi^2$  and a reasonable overall fit, we can extract the coupling constant  $g_{\phi N^* N}^2$  for all adopted  $N^*$ 's. The resultant  $g_{\phi N^* N}^2$ 's for these  $N^*$ 's are tabulated in Table II. The percentages of the individual contributions from all the considered  $N^*$ 's are given in the table as well.

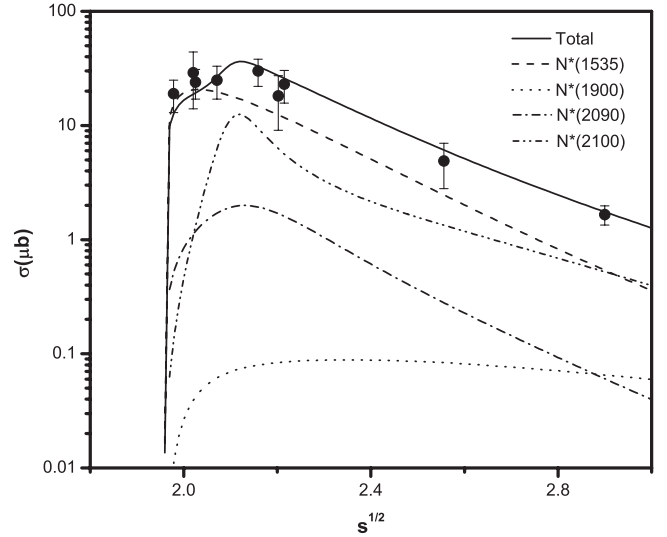
From this table, one has following observations: (1)  $N_{1/2^-}^*(1535)$  dominates the  $\pi^- p \rightarrow n\phi$  reaction and provides about 50% to 70% of the total contribution. This state may couple to  $N\phi$  strongly, and the coupling constant  $g_{\phi N^*(1535)N}^2$  ranges from 1.1 to 1.4. The contribution and the coupling to  $N\phi$  in type I is larger than those in type II.

(2) The  $N_{1/2}^*(2100)$  state is the second largest contributor and offers about 10% to 26% of the total contribution. It also shows that  $N_{1/2}^*(2100)$  may couple to  $N\phi$  remarkably. The value of the coupling constant  $g_{\phi N^*(2100)N}^2$  stretches from 0.09 to 0.19. And the contribution and the coupling to  $N\phi$  in type II is larger than those in type I. (3) The contribution from  $N_{1/2}^-(2090)$  is about 3% to 6%, and  $g_{\phi N^*(2090)N}^2$  spans a range from 0.007 to 0.014. The

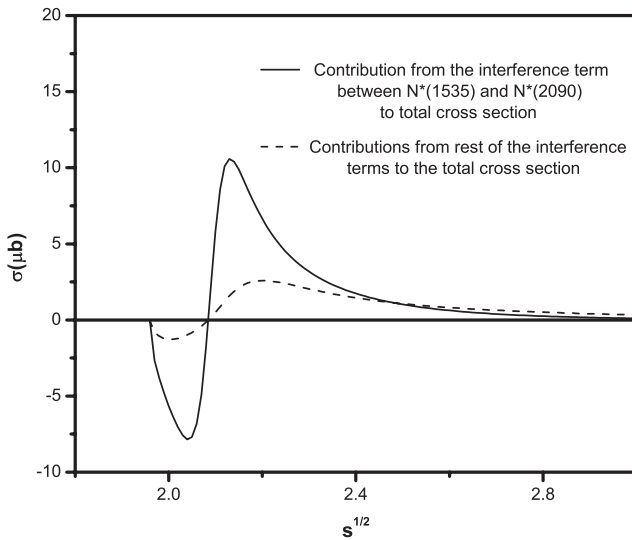
contribution and the coupling to  $N\phi$  in type I is slightly larger than those in type II. (4) The contribution from  $N_{3/2}^*(1900)$  is even smaller, about 0.4% to 1.0%, and  $g_{\phi N^*(1900)N}^2$  spreads in a range of 0.006 to 0.079. The effect from the uncertainty of the total width of this state is quite small. These observations are clearly consistent with the information from the curves shown in Fig. 3. Namely,  $N_{1/2}^*(2100)$  gives a contribution comparable to that from



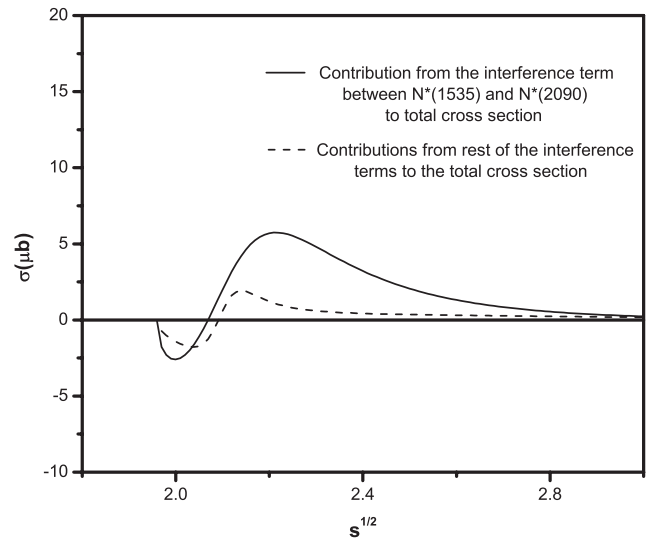
(a) Type I ( $\Gamma_{N^*(1900)}/\Gamma_{N^*(2090)}/\Gamma_{N^*(2100)} = 498\text{MeV}/95\text{MeV}/260\text{MeV}$ )



(b) Type II ( $\Gamma_{N^*(1900)}/\Gamma_{N^*(2090)}/\Gamma_{N^*(2100)} = 180\text{MeV}/350\text{MeV}/113\text{MeV}$ )



(c) Type I ( $\Gamma_{N^*(1900)}/\Gamma_{N^*(2090)}/\Gamma_{N^*(2100)} = 498\text{MeV}/95\text{MeV}/260\text{MeV}$ )



(d) Type II ( $\Gamma_{N^*(1900)}/\Gamma_{N^*(2090)}/\Gamma_{N^*(2100)} = 180\text{MeV}/350\text{MeV}/113\text{MeV}$ )

FIG. 3. Total cross section of the  $\pi^- p \rightarrow n\phi$  reaction. In Figs. (a) and (b), the solid curve describes the final fitting result, the dashed, dotted, dash-dotted, and dash-double-dotted curves denote the contributions from individual  $N_{1/2}^-(1535)$ ,  $N_{3/2}^*(1900)$ ,  $N_{1/2}^-(2090)$  and  $N_{1/2}^*(2100)$  states, respectively, and the solid dots with error bars are experimental data [14]. In Figs. (c) and (d), the solid and dashed curves represent the contributions from the interference term between  $N_{1/2}^-(1535)$  and  $N_{1/2}^-(2090)$  and the sum of the contributions from the rest of interference terms to the total cross section, respectively.

TABLE II. The extracted coupling constant  $g_{\phi NN}^2$  and the corresponding percentage of contribution in the  $\pi^- p \rightarrow n\phi$  reaction.

	$\Gamma_{N^*(1900)}/\Gamma_{N^*(2090)}/\Gamma_{N^*(2100)}$	$g_{\phi NN}^2(10^{-2})/(\text{fraction of contribution}(\%))$			
		$N_{1/2}^*(1535)$	$N_{3/2}^*(1900)$	$N_{1/2}^*(2090)$	$N_{1/2}^*(2100)$
Type I	180 MeV/95 MeV/200 MeV	140/67.1	7.92/0.9	0.937/3.6	12.3/13.5
	498 MeV/95 MeV/200 MeV	137/64.9	1.14/1.0	1.19/4.8	9.46/9.8
	180 MeV/95 MeV/260 MeV	128/61.7	3.53/0.4	1.37/5.6	10.8/15.4
	498 MeV/95 MeV/260 MeV	126/60.0	0.758/0.8	1.27/4.7	11.7/16.4
Type II	180 MeV/350 MeV/113 MeV	116/55.2	6.41/0.7	0.749/4.4	16.2/23.3
	498 MeV/350 MeV/113 MeV	115/52.6	0.656/0.7	0.967/5.4	17.0/23.1
	180 MeV/414 MeV/113 MeV	118/56.2	3.27/0.4	1.13/3.7	17.5/24.8
	498 MeV/414 MeV/113 MeV	114/54.0	0.783/0.7	1.05/3.3	18.6/25.7

$N_{1/2}^*(1535)$ , especially in the higher energy region,  $N_{1/2}^*(2090)$  offers a visible contribution around the energy about its mass, and  $N_{3/2}^*(1900)$  only provides a very small contribution in the whole energy region.

Next, we determine  $g_{\psi NN}^2$  in terms of the partial decay widths of the  $J/\psi \rightarrow p\bar{p}\eta$  and  $J/\psi \rightarrow p\bar{n}\pi^-$  processes, respectively. The partial wave analysis of the  $J/\psi \rightarrow p\bar{p}\eta$  data collected at BESII shows that the partial decay width from  $N_{1/2}^*(1535)$  is about  $(56 \pm 15)\%$  [11]. By fitting this width, one can easily obtain the magnitude of  $g_{\psi NN}^2(N_{1535})$ . Here we take the contribution of 56% in calculation. Again, a form factor with  $\Lambda$  being 1.8 GeV in Eq. (12) is adopted in the calculation to describe the off-shell effect of  $N_{1/2}^*(1535)$ . The extracted  $g_{\psi NN}^2(N_{1535})$  is tabulated in Table III. On the other hand, one notices that in analyzing the  $J/\psi \rightarrow p\bar{n}\pi^-$  data of BESII, assuming contributions from  $N_{3/2}^*(1900)$ ,  $N_{1/2}^*(2090)$  and  $N_{1/2}^*(2100)$  to be about 5 ~ 10%, respectively, are reasonable, and the resultant branching fraction of this channel is about  $(1.33 \pm 0.02(\text{stat.})) \times 10^{-3}$  [12]. Therefore, we can also assume that the contributions from  $N_{3/2}^*(1900)$ ,  $N_{1/2}^*(2090)$  and  $N_{1/2}^*(2100)$  are about 10%, 10% and 10%, respectively, in the  $J/\psi \rightarrow p\bar{n}\pi^-$  calculation. By using the extracted  $g_{\psi NN}^2$ 's and the form factor in Eq. (12) with  $\Lambda$  being

TABLE III.  $g_{\psi NN}^2$  and  $\Lambda$  for  $N_{1/2}^*(1535)$ ,  $N_{3/2}^*(1900)$ ,  $N_{1/2}^*(2090)$  and  $N_{1/2}^*(2100)$ .

$N^*$	Total width (GeV)	$g_{\psi NN}^2$	
		$\Lambda = 1.8 \text{ GeV}$	$\Lambda = 2.3 \text{ GeV}$
$N_{1/2}^*(1535)$	0.150	$1.319 \times 10^{-6}$	—
$N_{3/2}^*(1900)$	0.180	—	$2.422 \times 10^{-5}$
	0.498	—	$7.744 \times 10^{-6}$
$N_{1/2}^*(2090)$	0.095	—	$4.726 \times 10^{-5}$
	0.350	—	$1.612 \times 10^{-5}$
	0.414	—	$2.830 \times 10^{-5}$
$N_{1/2}^*(2100)$	0.113	—	$1.362 \times 10^{-5}$
	0.200	—	$2.290 \times 10^{-5}$
	0.260	—	$2.031 \times 10^{-5}$

2.3 GeV for either  $N_{3/2}^*(1900)$ , or  $N_{1/2}^*(2090)$  or  $N_{1/2}^*(2100)$ , we can extract  $g_{\psi NN}^2$  for these  $N^*$ 's from the the branching fraction of the  $J/\psi \rightarrow p\bar{n}\pi^-$  decay. The resultant  $g_{\psi NN}^2$  and corresponding  $\Lambda$  are tabulated in Table III. From this table, we find that  $g_{\psi NN}^2(N_{1535})$  is in the order of  $10^{-6}$ . Because of the uncertainties of the total width and corresponding  $g_{\pi NN}^2$  for  $N_{3/2}^*(1900)$ ,  $N_{1/2}^*(2090)$ , and  $N_{1/2}^*(2100)$ , the extracted  $g_{\psi NN}^2(N_{1900})$ ,  $g_{\psi NN}^2(N_{2090})$ , and  $g_{\psi NN}^2(N_{2100})$  would vary in the ranges of  $(0.77 \sim 2.4) \times 10^{-5}$ ,  $(1.6 \sim 4.7) \times 10^{-5}$ , and  $(1.4 \sim 2.3) \times 10^{-5}$ , respectively. It seems that the couplings of  $J/\psi$  to  $N$  and different  $N^*$ 's are about the same. This is understandable, because that  $J/\psi$  is merely composed of charmed quarks,  $N$  consists of upper and down quarks only, and  $N^*$  is made up of upper, down and even strange quarks, thus the coupling mechanisms for different  $N^*$ 's would be the same.

In terms of the extracted  $g_{\psi NN}^2$  and  $g_{\phi NN}^2$ , we are in the stage of calculating physics observables in the  $J/\psi \rightarrow p\bar{p}\phi$  decay with the adoption of  $N_{1/2}^*(1535)$ ,  $N_{3/2}^*(1900)$ ,  $N_{1/2}^*(2090)$ , and  $N_{1/2}^*(2100)$ . The resultant  $p\phi$  invariant mass spectra are plotted in Fig. 4. In Figs. 4(a) and 4(b), the dashed and solid curves represent the upper and lower bounds, which are caused by the uncertainties of the widths of the  $N_{3/2}^*(1900)$ ,  $N_{1/2}^*(2090)$  and  $N_{1/2}^*(2100)$  states, in type I and type II cases, respectively. And in Figs. 4(c) and 4(d), the dashed, dotted, dash-dotted, and dash-double-dotted curves describe the subcontributions from the  $N_{1/2}^*(1535)$ ,  $N_{3/2}^*(1900)$ ,  $N_{1/2}^*(2090)$  and  $N_{1/2}^*(2100)$  states in these two cases, respectively.

The percentages of various  $N^*$ 's contributions in the decay process are tabulated in Table IV. From the numerical values in Table IV and the  $p\phi$  invariant mass curves in Fig. 4, we have following observations. From Fig. 4(a), and Table IV one sees that in type I the contribution from  $N_{1/2}^*(2090)$  is about (46.3 ~ 72.1)%, and there is a peak structure around 2.09 GeV. The subcontributions in Fig. 4(c) tell us that this structure is mainly contributed by  $N_{1/2}^*(2090)$  due to its relatively narrow width, namely,

a stronger coupling between  $N$  and  $\phi$ . This implies that there may exist a large  $N\phi$  or  $qqqs\bar{s}$  component in  $N_{1/2}^*(2090)$ . Meanwhile the  $N_{1/2}^*(2100)$  state also provides a sizable contribution of about (15.1 ~ 32.8)%, but this contribution is smaller than that offered by  $N_{1/2}^*(2090)$ , and the shape of the contribution is flatter due to a large width of the state.

Therefore, this piece of contribution would not affect the shape of the total contribution qualitatively. The contributions from  $N_{1/2}^*(1535)$  and  $N_{3/2}^*(1900)$  are negligibly small, their contributions are about (1.81 ~ 2.00)% and (0.01 ~ 0.44)%, respectively. The interference terms can only provide about 2% of the total contribution. Therefore, disregarding the contributions from the  $N_{1/2}^*(1535)$  and

$N_{3/2}^*(1900)$  states and the interference terms will not affect the conclusion qualitatively. From Fig. 4(b) and Table IV, one finds that in type II the contribution from  $N_{1/2}^*(2100)$  is about (76.3 ~ 87.6)%, and there is also a small peak structure around 2.11 GeV. The subcontributions in Fig. 4(d) show that this structure is almost entirely contributed by  $N_{1/2}^*(2100)$ , because of its dominant contribution and relatively narrow width. This also implies that  $N_{1/2}^*(2100)$  may couple to  $N\phi$  remarkably, and a significant  $N\phi$  or  $qqqs\bar{s}$  component may exist in this state. Meanwhile the contributions from  $N_{1/2}^*(1535)$ ,  $N_{3/2}^*(1900)$  and  $N_{1/2}^*(2090)$  are negligibly small, their contributions are about (1.63 ~ 1.70)%, (0.01 ~ 0.36)% and (1.33 ~ 2.65)%, respectively. The interference terms

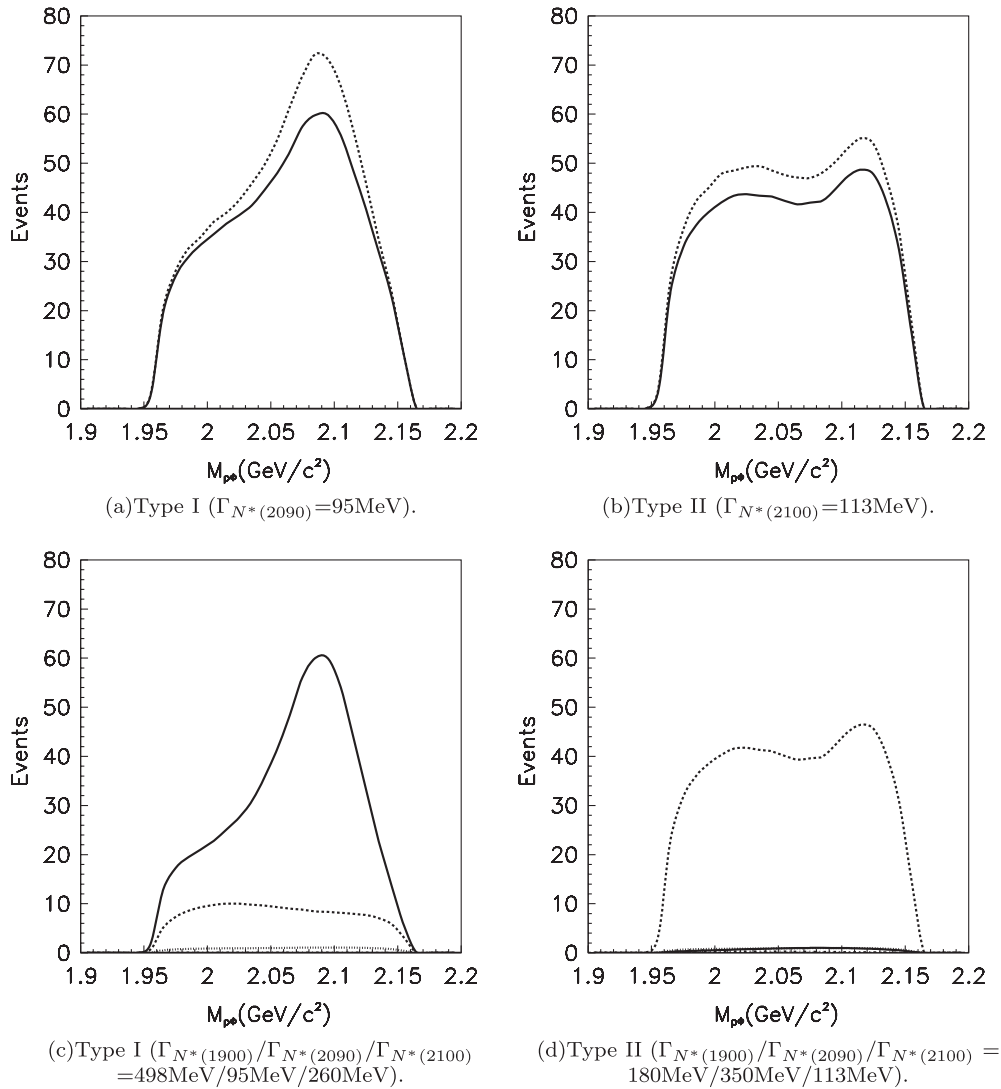


FIG. 4.  $p\phi$  invariant mass spectra in the  $J/\psi \rightarrow p\bar{p}\phi$  decay. (a) and (b) describe the upper (dashed curve) and lower (solid curve) bounds in the type I ( $\Gamma_{N^*(2100)} = 113 \text{ MeV}$ ) and type II ( $\Gamma_{N^*(2090)} = 95 \text{ MeV}$ ) cases, respectively. (c) and (d) show the subcontributions from  $N^*(2090)$  (solid curve),  $N^*(2100)$  (dashed curve),  $N^*(1535)$  (dash-dotted curve) and  $N^*(1900)$  (dash-double-dotted curve) in type I and type II cases, respectively.



TABLE IV. Percentages of contributions from  $N_{1/2}^*(1535)$ ,  $N_{3/2}^*(1900)$ ,  $N_{1/2}^*(2090)$  and  $N_{1/2}^*(2100)$  in the  $J/\psi \rightarrow p\bar{p}\phi$  decay.

	$\Gamma_{N^*(1900)}/\Gamma_{N^*(2090)}/\Gamma_{N^*(2100)}$	Fraction(%)			
		$N^*(1535)$	$N^*(1900)$	$N^*(2090)$	$N^*(2100)$
Type I	180 MeV/95 MeV/200 MeV	2.01	0.44	48.22	32.80
	498 MeV/95 MeV/200 MeV	1.96	0.01	61.24	25.23
	180 MeV/95 MeV/260 MeV	1.83	0.20	70.51	15.12
	498 MeV/95 MeV/260 MeV	1.81	0.01	65.36	16.38
Type II	180 MeV/350 MeV/113 MeV	1.66	0.36	1.42	76.26
	498 MeV/350 MeV/113 MeV	1.65	0.01	1.83	80.03
	180 MeV/414 MeV/113 MeV	1.69	0.18	2.72	82.38
	498 MeV/414 MeV/113 MeV	1.63	0.01	2.53	87.56

can only give a contribution about 2%. These results also imply that one would not be able to explore the possible strange structures for  $N_{1/2}^*(1535)$  and  $N_{3/2}^*(1900)$  in the type I case and for  $N_{1/2}^*(1535)$ ,  $N_{3/2}^*(1900)$  and  $N_{1/2}^*(2090)$  in the type II case in this decay process, because their informations are deeply submerged in the signals of the  $N_{1/2}^*(2090)$  and  $N_{1/2}^*(2100)$  states and the  $N_{1/2}^*(2100)$  state, respectively.

Furthermore, the Dalitz plots for type I and type II are plotted in Fig. 5. They have distinguishable features. In the type I case, there are one vertical belt and one horizontal belt at  $4.37(\text{GeV}/c^2)^2$  and an enhancement in the upper right corner. But in the type II case, there are only two enhancements at the upper left and lower right corners. These patterns agree with the findings from the invariant mass curves.

Finally, we need to mention that the value of the cutoff parameter in a certain range does not qualitatively affect our conclusion.

#### IV. SUMMARY

In this paper, the  $J/\psi \rightarrow p\bar{p}\phi$  decay is studied in an isobar resonance model with effective Lagrangians. Because of the  $s\bar{s}$  structure of the  $\phi$ -meson and the Okubo-Zweig-Iizuka rule, the major contribution to this process is expected to come from intermediate  $N^*$  resonances containing significant strangeness. Therefore, this decay process could be used to explore the possible strangeness structure of the  $N^*$  resonances.

Based on a careful analysis, four PDG listed  $N^*$  states,  $N_{1/2}^*(1535)$ ,  $N_{3/2}^*(1900)$ ,  $N_{1/2}^*(2090)$  and  $N_{1/2}^*(2100)$ , are expected to give major contribution to this decay and

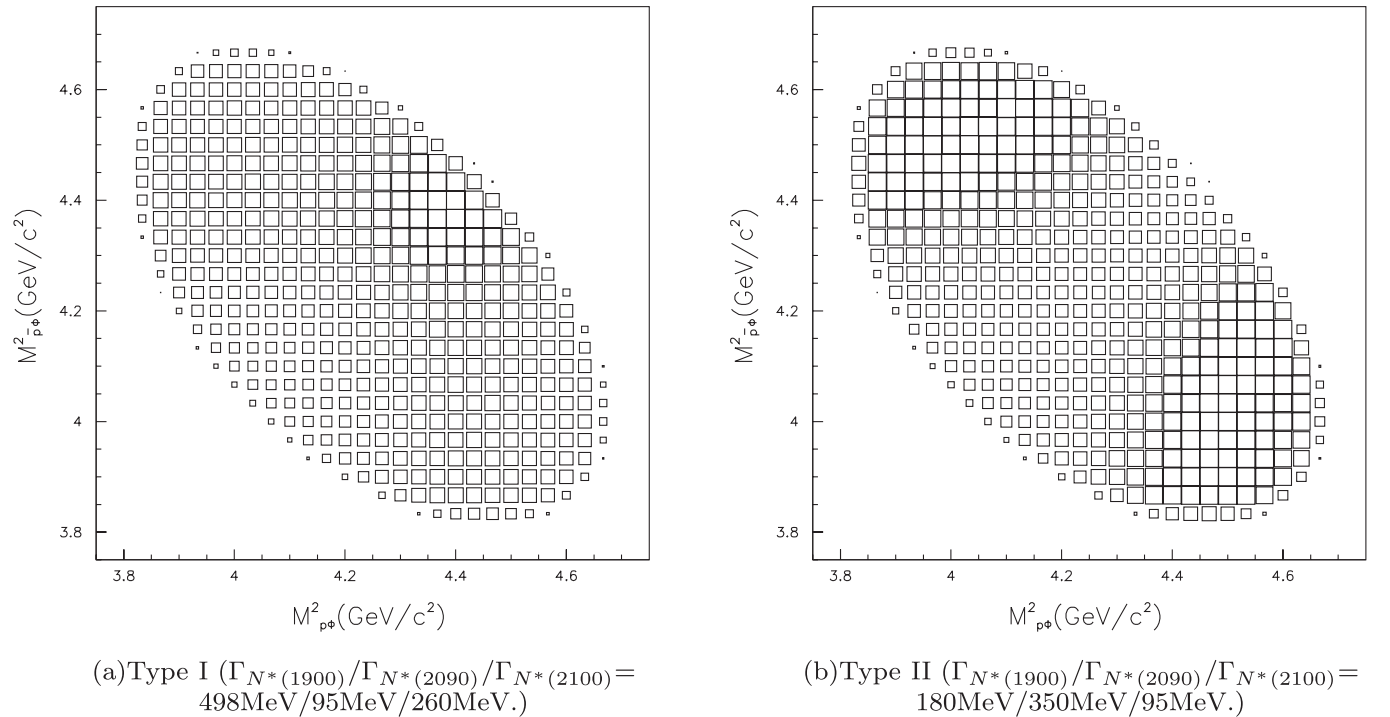


FIG. 5. Dalitz plots.

hence adopted in the calculation. The coupling constants  $g_{\pi NN^*}^2$  for these  $N^*$ 's and  $g_{\eta NN^*}^2$  for  $N_{1/2^-}^*(1535)$  are extracted from their relevant branching fractions. With the determined  $g_{\pi NN^*}^2$ , coupling constant  $g_{\phi NN^*}^2$  for  $N^*$ 's are obtained by fitting the cross section of the  $\pi^- p \rightarrow n\phi$  reaction. Because of the uncertainties of the partial width for  $N_{3/2^+}^*(1900)$ ,  $N_{1/2^-}^*(2090)$  and  $N_{1/2^+}^*(2100)$ , the resultant  $g_{\phi NN^*}^2$ 's are allowed to change in certain regions. It is found that in the best fit, except the dominant contribution from  $N_{1/2^-}^*(1535)$  and negligible contribution from  $N_{3/2^+}^*(1900)$ , the contributions from  $N_{1/2^-}^*(2090)$  and  $N_{1/2^+}^*(2100)$  are visible and even remarkable in some cases, and the total widths of these two states cannot be large simultaneously. Therefore, there are two types of fits. In the first type, type I,  $N_{1/2^-}^*(2090)$  has a smaller total width while  $N_{1/2^+}^*(2100)$  has a larger total width; and in the second type, type II, it is the other way round. Then, the coupling constant  $g_{\psi NN^*(1535)}^2$  and  $g_{\psi NN^*}^2$  for other three  $N^*$ 's are extracted by fitting the partial decay widths of the  $J/\psi \rightarrow p\bar{p}\eta$  process and the  $J/\psi \rightarrow p\bar{n}\pi^-$  process, respectively.

Finally, we calculate the physical observables in the  $J/\psi \rightarrow p\bar{p}\phi$  decay by using obtained  $g_{\pi NN^*}^2$ 's and  $g_{\psi NN^*}^2$ 's in the type I and type II cases. The invariant mass spectrum of  $p\phi$  in the type I case shows that there is a peak structure around 2.09 GeV due to the major contribution from the narrower  $N_{1/2^-}^*(2090)$  state. This means that its coupling to  $N\phi$  is relatively strong, and a large  $N\phi$  or  $qqqs\bar{s}$  component may exist in  $N_{1/2^-}^*(2090)$ . Meanwhile the contribution from  $N_{1/2^+}^*(2100)$  is flatter and smaller, which implies that even there is a strange ingredient in this state, its coupling to  $N\phi$  would be weaker. In the type II case, the curve of the invariant mass spectrum of  $p\phi$  has a small peak structure around 2.11 GeV, because of the dominant contribution from the narrow  $N_{1/2^+}^*(2100)$

state and negligible contributions from other states. It suggests that its coupling to  $N\phi$  may be strong, a significant  $N\phi$  or  $qqqs\bar{s}$  component might exist in the  $N_{1/2^+}^*(2100)$ . However, one would not be able to reveal the strange structure in  $N_{1/2^-}^*(2090)$ , because its information is deeply submerged in the signal of the  $N_{1/2^+}^*(2100)$  state.

In summary, in the  $J/\psi \rightarrow p\bar{p}\phi$  decay, the widths of  $N_{1/2^-}^*(2090)$  and  $N_{1/2^+}^*(2100)$  cannot be large simultaneously. The proposed study of this channel with the high statistics BESIII data [20] will tell us how the  $p\phi$  invariant mass curve goes. If the shape of the curve likes that of type I, the width of the  $N_{1/2^-}^*(2090)$  state is narrower and there would be a considerable amount of  $p\phi$  or  $qqqs\bar{s}$  component in the state, while the width of the  $N_{1/2^+}^*(2100)$  state would be wider. If the shape of the curve is similar to that of type II, only the width of the  $N_{1/2^+}^*(2100)$  state is relatively narrow and a certain amount of  $p\phi$  or  $qqqs\bar{s}$  component might exist in the state. Of course, the BESIII data with high statistics on the  $J/\psi \rightarrow p\bar{p}\phi$  decay would provide more knowledge about all possible  $N^*$ 's than our predictions based on the information from  $\pi N \rightarrow \phi N$ . It will definitely reveal useful information for those  $N^*$  resonances which have large  $qqqs\bar{s}$  component. And the  $pp \rightarrow pp\phi$  reaction should also be studied to check our prediction.

## ACKNOWLEDGMENTS

This work is partly supported by the National Natural Science Foundation of China under Grant Nos. 10875133, 11105126, 10975038, 11035006, 11165005, and the Key-project by the Chinese Academy of Sciences under Project No. KJCX2-EW-N01, and the Ministry of Science and Technology of China (2009CB825200).

- 
- [1] B.C. Liu and B.S. Zou, *Phys. Rev. Lett.* **96**, 042002 (2006); **98**, 039102 (2007).
  - [2] B.C. Liu and B.S. Zou, *Commun. Theor. Phys.* **46**, 501 (2006).
  - [3] G. Penner and U. Mosel, *Phys. Rev. C* **66**, 055211 (2002); **66**, 055212 (2002); V. Shklyar, H. Lenske, and U. Mosel, *Phys. Rev. C* **72**, 015210 (2005).
  - [4] B. Julia-Diaz, B. Saghai, T.S.H. Lee, and F. Tabakin, *Phys. Rev. C* **73**, 055204 (2006).
  - [5] M.Q. Tran *et al.*, *Phys. Lett. B* **445**, 20 (1998); K.H. Glander *et al.*, *Eur. Phys. J. A* **19**, 251 (2004).
  - [6] J.W.C. McNabb *et al.* (CLAS Collaboration), *Phys. Rev. C* **69**, 042201(R) (2004).
  - [7] S. Okubo, *Phys. Lett.* **5**, 165 (1963); G. Zweig, CERN Report No. Th-412 (unpublished); J. Iizuka, *Prog. Theor. Phys. Suppl.* **37**, 21 (1966).
  - [8] J.J. Xie, B.S. Zou, and H.C. Chiang, *Phys. Rev. C* **77**, 015206 (2008) and references therein.
  - [9] The Review of Particle Physics, C. Amsler *et al.*, *Phys. Lett. B* **667**, 1 (2008).
  - [10] J.E. Augusttin *et al.* (DM2 Collaboration), *Phys. Rev. Lett.* **60**, 2238 (1988).
  - [11] J.Z. Bai *et al.* (BES Collaboration), *Phys. Lett. B* **510**, 75 (2001).
  - [12] M. Ablikim *et al.* (BES Collaboration), *Phys. Rev. Lett.* **97**, 062001 (2006).

- [13] A. Sibirtsev, J. Haidenbauer, and U.-G. Meissner, *Eur. Phys. J. A* **27**, 263 (2006); A. Sibirtsev and W. Cassing, *ibid.* **7**, 407 (2000); A.I. Titov, B. Kämpfer, and B.L. Reznik, *Eur. Phys. J. A* **7**, 543 (2000); K. Tsushima and K. Nakayama, *Phys. Rev. C* **68**, 034612 (2003); L.P. Kaptari and B. Kämpfer, *Eur. Phys. J. A* **23**, 291 (2004).
- [14] A. Baldini *et al.*, *Total Cross Sections of High Energy Particles: Landolt-Börnstein, Numerical Data and Functional Relationships in an Technology*, edited by H. Schopper (Springer-Verlag, New York, 1988), Vol. 12.
- [15] K. Tsushima, A. Sibirtsev, and A. W. Thomas, *Phys. Lett. B* **390**, 29 (1997) and references therein.
- [16] A.I. Titov, B. Kämpfer, and B.L. Reznik, *Phys. Rev. C* **65**, 065022 (2002) and references therein.
- [17] G. Penner and U. Mosel, *Phys. Rev. C* **66**, 055211 (2002); **66**, 055212 (2002); V. Shklyar, H. Lenske, and U. Mosel, *Phys. Rev. C* **72**, 015210 (2005).
- [18] T. Feuster and U. Mosel, *Phys. Rev. C* **58**, 457 (1998); **59**, 460 (1999).
- [19] W.H. Liang *et al.*, *J. Phys. G* **28**, 333 (2002).
- [20] D.M. Asner *et al.*, *Int. J. Mod. Phys. A* **24**, 499 (2009); private talk with H.C. Chiang and W.H. Liang, 2007.